DTU Library

Acoustofluidics 1: Governing equations in microfluidics

Bruus, Henrik

Published in:
Lab on a Chip

Link to article, DOI:
[10.1039/c1lc20658c](#)

Publication date:
2011

Document Version
Publisher's PDF, also known as Version of record

[Link back to DTU Orbit](#)

Citation (APA):
Bruus, H. (2011). Acoustofluidics 1: Governing equations in microfluidics. *Lab on a Chip*, *11*(22), 3742-3751. https://doi.org/10.1039/c1lc20658c

FOCUS

Acoustofluidics 1: Governing equations in microfluidics

Henrik Bruus

In Part 1 of the thematic tutorial series "*Acoustofluidics – exploiting ultrasonic standing waves forces and acoustic streaming in microfluidic systems for cell and particle manipulation*", we establish the governing equations in microfluidics. Examples of basic flow solutions are presented, and equivalent circuit modeling for determining flow rates in microfluidic networks is introduced.

I.   Introduction

Microfluidics deals with the flow of fluids and suspensions in channels of sub-milli-metre-sized cross-sections under the influence of external forces.[1–6] Here, viscosity

Department of Micro- and Nanotechnology, Technical University of Denmark DTU Nanotech, Building 345 B, DK-2800, Kongens Lyngby, Denmark

dominates over inertia, ensuring the absence of turbulence and the appearance of regular and predictable laminar flow streams, which implies an exceptional spatial and temporal control of solutes. The combination of laminar flow streams and precise control of external forces acting on particles in solution, has resulted in particle handling methods useful for analytical chemistry and bioanalysis, based on different physical mechanisms including inertia,[7] electrokinetics,[8] dielectropho-retics,[9] magnetophoretics,[10] as well as mechanical contact forces.[11]

Acoustofluidics, *i.e.* ultrasound-based external forcing of microparticles in microfluidics, has attracted particular attention because it allows gentle, label-free separation based on purely mechanical properties: size, shape, density, and compressibility. The early acousto-phoretic microparticle filters[12–16] were soon developed into the first successful

on-chip acoustophoretic separation devices.[17,18] Many different biotechnical applications of acoustophoresis have subsequently emerged including cell trapping,[19–21] plasmapheresis,[22] forensic analysis,[23] food analysis,[24] cell sorting using surface acoustic waves,[25] cell synchronization,[26] and cell differentia-tion.[27] Furthermore, substantial advancements in understanding the fundamental physics of microsystems acoustophoresis have been achieved through full-chip imaging of acoustic resonances,[28] surface acoustic wave generation of standing waves,[29] multi-resonance chips,[30] advanced frequency control,[31,32] on-chip integration with magnetic separators,[33] acoustics-assisted microgrippers,[34] *in situ* force calibration,[35] and automated systems.[36]

In Part 1 of the Acoustofluidics Tutorial Series we study the governing equations in microfluidics formulated in terms of the classical continuum field description of velocity $\boldsymbol{v}$, pressure p, and density ρ. We also present some of the basic flow solutions as well as the equivalent circuit modeling useful for predicting the flow rates through networks of microfluidic channels.

II.   The basic continuum fields

In the following we use the so-called Eulerian picture of the continuum fields, where the spatial coordinates $\boldsymbol{r}$ are fixed in space, and where we observe how the fields evolve in time at these points. Consequently, the position $\boldsymbol{r}$ and the time t are independent variables. The Eulerian picture is illustrated by the velocity field in Fig. 1. In general, the value of any field variable $F(\boldsymbol{r}, t)$ is defined as the average

Henrik Bruus

Prof. Henrik Bruus received his B.Sc. in mathematics and physics from the University of Copenhagen in 1984 and his M.Sc. and Ph.D. degrees in physics from the Niels Bohr Institute, University of Copenhagen in 1986 and 1990, respectively. He was postdoctoral fellow at Nordic Institute of Theoretical Physics 1990–92, Yale University 1992–94 and CNRS Grenoble 1994–96. He returned to the Niels Bohr Institute as an associate professor 1997–2001, before he joined the faculty at DTU Nanotech, Technical University of Denmark in 2002. He was promoted full professor there in 2005. He has (co)authored more than 90 peer-reviewed journal papers on condensed matter physics and microfluidics, as well as 110 peer-re-viewed conference contributions and 2 monographs, the latest being "Theoretical Microfluidics", Oxford University Press (2008).
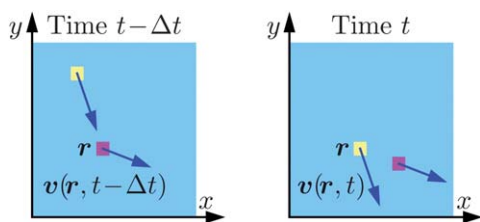
Fig. 1 The Eulerian picture: the spatial coordinates r do not follow the flow. Instead, the velocity field $\mathbf{v}$ at the fixed point r is defined by the molecules in the purple region at time $t - \Delta t$, and by those in the yellow region at time t.

value $\langle F_{\mathrm{mol}}(\mathbf{r}', t) \rangle$ of the corresponding molecular quantity for all the molecules contained in some liquid particle of volume $\Delta V(\mathbf{r})$ around $\mathbf{r}$ at time t,

$$F(\mathbf{r}, t) = \langle F_{\mathrm{mol}}(\mathbf{r}', t) \rangle_{\mathbf{r}' \in \Delta V(\mathbf{r})}. \quad (1)$$

If we for brevity let m_i and v_i be the mass and the velocity of molecule i, respectively, and furthermore let $i \in \Delta V$ stand for all molecules i present inside the volume $\Delta V(\mathbf{r})$ at time t, then the definition of the density $\rho(\mathbf{r}, t)$ and the velocity field $\mathbf{v}(\mathbf{r}, t)$ can be written as

$$\rho(\mathbf{r}, t) \equiv \frac{1}{\Delta V} \sum_{i \in \Delta V} m_i, \quad (2a)$$

$$\mathbf{v}(\mathbf{r}, t) \equiv \frac{1}{\rho(\mathbf{r}, t)\Delta V} \sum_{i \in \Delta V} m_i v_i. \quad (2b)$$

Here, we have introduced the sign "$\equiv$" for "equal-to-by-definition sign". Notice how the velocity is defined through the more fundamental concept of momentum.

The dependent field variables in microfluidics can be scalars (such as density ρ, viscosity η, pressure p, temperature T, and free energy $\mathcal{F}$), vectors (such as velocity $\mathbf{v}$, current density $\mathbf{J}$, pressure gradient ∇p, force density $\mathbf{f}$, and electric field $\mathbf{E}$), and tensors (such as stress tensor $\boldsymbol{\sigma}$ and velocity gradient $\nabla \mathbf{v}$).

III. Mathematical notation

The mathematical treatment of microfluidic problems is complicated due to the presence of several scalar, vector and tensor fields and the non-linear partial differential equations that govern them. To facilitate the treatment some simplifying notation is called for. We follow ref. 4.

First, a suitable co-ordinate system must be chosen. We shall mainly work

with Cartesian co-ordinates (x, y, z) with corresponding basis vectors $\mathbf{e}_x$, $\mathbf{e}_y$, and $\mathbf{e}_z$ of unity length and mutually orthogonal. The position vector $\mathbf{r} = (r_x, r_y, r_z) = (x, y, z)$ is written as

$$\mathbf{r} = r_x \mathbf{e}_x + r_y \mathbf{e}_y + r_z \mathbf{e}_z = x\mathbf{e}_x + y\mathbf{e}_y + z\mathbf{e}_z. \quad (3)$$

Any vector $\mathbf{v}$ can be written in terms of its components v_i (where for Cartesian co-ordinates $i = x, y, z$) as

$$\mathbf{v} = \sum_{i=x,y,z} v_i \mathbf{e}_i \equiv v_i \mathbf{e}_i. \quad (4)$$

In the last equality we have introduced the Einstein summation convention: a repeated index implies a summation over that index (unless noted otherwise). Other examples of this compact, so-called index notation, is the vector scalar product $\mathbf{u} \cdot \mathbf{v}$, the length v of a vector $\mathbf{v}$, and the ith component of the matrix equation $\mathbf{u} = M\mathbf{v}$,

$$\mathbf{v} \cdot \mathbf{u} = v_i u_i, \quad (5a)$$

$$v = |\mathbf{v}| = \sqrt{\mathbf{v}^2} = \sqrt{\mathbf{v} \cdot \mathbf{v}} = \sqrt{v_i v_i}, \quad (5b)$$

$$u_i = M_{ij} v_j. \quad (5c)$$

For the partial derivatives of a given function $F(\mathbf{r}, t)$ we use the symbols ∂_i, with $i = x, y, z$, and ∂_t,

$$\partial_x F \equiv \frac{\partial F}{\partial x}, \quad \text{and} \quad \partial_t F \equiv \frac{\partial F}{\partial t}. \quad (6)$$

The vector differential operator nabla ∇ contains the three partial space derivatives ∂_i. It plays an important role in differential calculus, and it is defined by

$$\nabla \equiv \mathbf{e}_x \partial_x + \mathbf{e}_y \partial_y + \mathbf{e}_z \partial_z = \mathbf{e}_i \partial_i. \quad (7)$$

The Laplace operator, which appears in numerous partial differential equations in theoretical physics, is just the square of the nabla operator,

$$\nabla \cdot \nabla \equiv \nabla^2 \equiv \partial_i \partial_i. \quad (8)$$

In terms of ∇ the total time derivative of a quantity $F(\mathbf{r}(t), t)$ flowing along with the fluid can be written as

$$\frac{\mathrm{d}F}{\mathrm{d}t} = \partial_t F + (\partial_t r_i)\partial_i F = \partial_t F + (\mathbf{v} \cdot \nabla)F. \quad (9)$$

Since ∇ is a differential operator, the order of the factors does matter in a scalar product containing it. So, whereas $\mathbf{v} \cdot \nabla$ in the previous equation is a scalar differential operator, the product $\nabla \cdot \mathbf{v}$ with the reversed order of the factors is a scalar function. The latter appears so often in mathematical physics that it has acquired its own name, namely the divergence of the vector field,

$$\nabla \cdot \mathbf{v} \equiv \partial_x v_x + \partial_y v_y + \partial_z v_z = \partial_i v_i. \quad (10)$$

Concerning integrals, we denote the 3D integral measure by $\mathrm{d}\mathbf{r}$, so that in Cartesian co-ordinates we have $\mathrm{d}\mathbf{r} = \mathrm{d}x \, \mathrm{d}y \, \mathrm{d}z$. We also consider definite integrals as operators acting on integrands, thus we keep the integral sign and the associated integral measure together to the left of the integrand. As an example, the integral in spherical coordinates (r, θ, ϕ) over a spherical body with radius a of the scalar function $S(\mathbf{r})$ is written as

$$\int_{\mathrm{sphere}} \mathrm{d}x \, \mathrm{d}y \, \mathrm{d}z \, S(x, y, z) = \int_{\mathrm{sphere}} \mathrm{d}\mathbf{r} \, S(\mathbf{r})$$
$$= \int_0^a r^2 \mathrm{d}r \int_0^\pi \sin\theta d\theta \int_0^{2\pi} \mathrm{d}\phi \, S(r, \theta, \phi). \quad (11)$$

When working with vectors and tensors it is advantageous to use the following two special symbols: the Kronecker delta δ_{ij} and and the Levi-Civita symbol ε_{ijk},

$$\delta_{ij} = \begin{cases} 1, & \text{for } i = j, \\ 0, & \text{for } i \neq j, \end{cases} \quad (12a)$$

$$\varepsilon_{ijk} = \begin{cases} +1, & \text{if } (ijk) \text{ is an even} \\ & \text{permutation of } (xyz), \\ -1, & \text{if } (ijk) \text{ is an odd} \\ & \text{permutation of } (xyz), \\ 0, & \text{otherwise.} \end{cases} \quad (12b)$$

In the index notation, the Levi-Cevita symbol appears directly in the definition of the ith component of the cross-product

$u \times v$ of two vectors u and v, and of the rotation $\nabla \times v$,

$$(u \times v)_i \equiv \varepsilon_{ijk} u_j v_k, \text{ and } (\nabla \times v)_i \equiv \varepsilon_{ijk} \partial_j v_k. \quad (13)$$

When evaluating the rotation of a rotation, the "pairing-minus-antipairing" theorem is very useful,

$$\varepsilon_{ijk} \varepsilon_{ilm} = \delta_{jl} \delta_{km} - \delta_{jm} \delta_{kl}. \quad (14)$$

As a last mathematical subject, we mention Gauss's theorem, which we shall employ repeatedly below. For a given vector field $V(r)$, it relates the volume integral in a given region Ω of the divergence $\nabla \cdot V$ to the integral over the surface $\partial\Omega$ of the flux $V \cdot n$ da through an area element da with the surface normal n,

$$\int_{\Omega} dr \, \nabla \cdot V = \int_{\partial\Omega} da \, n \cdot V,$$

$$\text{or} \int_{\Omega} dr \, \partial_j V_j = \int_{\partial\Omega} da \, n_j V_j. \quad (15)$$

By definition, the surface normal n of a closed surface is an outward-pointing unit vector perpendicular to the surface, hence the name *divergence*. For a tensor T_{jk} of rank 2 the theorem states $\int_{\Omega} dr \, \partial_j T_{jk} = \int_{\partial\Omega} da \, n_j T_{jk}$ with a straightforward generalization to higher ranks.

IV. Governing equations

A. The continuity equation

The first governing equation to be derived is the continuity equation, which expresses the conservation of mass. We consider a compressible fluid, *i.e.* the density ρ may vary as function of space
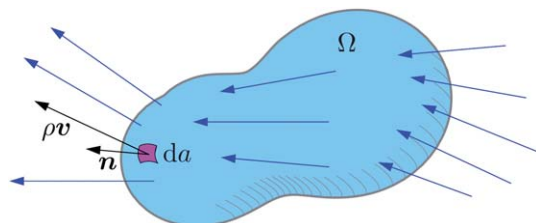

Fig. 2 A sketch of the mass current density field ρv (long arrows) flowing through an arbitrarily shaped, but fixed region Ω (blue). Any infinitesimal area da (purple) is associated with an outward-pointing unit vector n (short arrow) perpendicular to the local surface. The current flowing out through the area da is given by da times the projection $\rho v \cdot n$ of the current density on the surface unit vector.

and time, and a fixed, arbitrarily shaped region Ω in the fluid as sketched in Fig. 2. The total mass $M(\Omega, t)$ inside Ω can be expressed as a volume integral over the density ρ,

$$M(\Omega, t) = \int_{\Omega} dr \rho(r, t). \quad (16)$$

Since mass can neither appear nor disappear spontaneously in non-relativistic mechanics, $M(\Omega, t)$ can only vary due to a mass flux through the surface $\partial\Omega$ of the region Ω. The mass current density J is defined as the mass density ρ times the advection velocity v, *i.e.* the mass flow per oriented area per time (kg m^{-2} s^{-1}),

$$J(r, t) = \rho(r, t) \, v(r, t). \quad (17)$$

As the region Ω is fixed $\partial_t M(\Omega, t)$ can be calculated either by differentiating the volume integral eqn (16),

$$\partial_t M(\Omega, t) = \partial_t \int_{\Omega} dr \rho(r, t)$$
$$= \int_{\Omega} dr \, \partial_t \rho(r, t), \quad (18)$$

or as a surface integral over $\partial\Omega$ of the mass current density using eqn (17) and Fig. 2,

$$\partial_t M(\Omega, t) = \int_{\partial\Omega} da(-n) \cdot J$$
$$= -\int_{\partial\Omega} da \, n \cdot (\rho v)$$
$$= -\int_{\Omega} dr \, \nabla \cdot [\rho(r, t) v(r, t)]. \quad (19)$$

The last expression is obtained by applying Gauss's theorem eqn (15) to the vector field $V \equiv \rho v$. We have used $-n$ because this is the direction of *entering* the region. It follows immediately from eqn (18) and (19) that

$$\int_{\Omega} dr \, \partial_t \rho(r, t) = -\int_{\Omega} dr \, \nabla \cdot [\rho(r, t) v(r, t)]. \quad (20)$$

This result is true for any choice of region Ω. However, this is only possible if the integrands are identical. Thus we have derived the continuity equation,

$$\partial_t \rho = -\nabla \cdot (\rho v) \text{ or } \partial_t \rho = -\partial_j (\rho v_j). \quad (21)$$

In many cases, especially in microfluidics, where the flow velocity is much smaller than the velocity of speed of sound (pressure waves), the fluid appears incompressible. Thus, ρ is constant in space and time, and the continuity equation simplifies to,

$$\nabla \cdot v = 0 \text{ or } \partial_i v_i = 0. \quad (22)$$

In Part 2 of the Tutorial Series,[37] compressibility $\rho = \rho(p)$ will be discussed further in connection with acoustics.

B. The Navier–Stokes equation

The second governing equation, the Navier–Stokes equation, is the equation of motion for the Eulerian velocity field directly related to momentum conservation and the momentum density ρv. It is derived using an approach similar to that which led us to the continuity equation. We consider the ith component $P_i(\Omega, t)$ of the total momentum of the fluid inside an arbitrarily shaped, but fixed, region Ω. In analogy with the mass eqn (18), the rate of change of the momentum is given by

$$\partial_t P_i = \partial_t \int_{\Omega} dr \rho(r, t) v_i(r, t)$$
$$= \int_{\Omega} dr [(\partial_t \rho) v_i + \rho \partial_t v_i]. \quad (23)$$

In contrast to the mass inside Ω, which according to eqn (19) can only change by advection through the surface $\partial\Omega$, the momentum $P_i(\Omega, t)$ can change both by advection and by the action of forces given by Newton's second law. These forces can be divided into body forces that act on the interior of Ω, *e.g.* gravitational and electrical forces, and contact forces that act on the surface $\partial\Omega$ of Ω, *e.g.* pressure and viscosity forces. Thus, the rate of change of the ith component of the momentum can be written as

$$\partial_t P_i = \partial_t P_i^{\text{body}} + \partial_t P_i^{\text{adv}} + \partial_t P_i^{\text{pres}} + \partial_t P_i^{\text{visc}}. \quad (24)$$

A body force $\boldsymbol{f}^{\text{body}}$ is an external force that acts throughout the entire body of the fluid. The change in the momentum of Ω due to $\boldsymbol{f}^{\text{body}}$, e.g. gravity in terms of the density ρ and the acceleration of gravity $\boldsymbol{g}$, is

$$\partial_t P_i^{\text{body}} = \int_\Omega d\boldsymbol{r}\, f_i^{\text{body}} = \int_\Omega d\boldsymbol{r}(\rho \boldsymbol{g})_i$$
$$= \int_\Omega d\boldsymbol{r}\, \rho g_i. \quad (25)$$

For the advection of momentum $\rho \boldsymbol{v}$ into Ω, we note that it is described in terms of the tensor $(\rho \boldsymbol{v})\boldsymbol{v}$, just as advection of density ρ is described by the vector $(\rho)\boldsymbol{v}$. Considering the ith momentum component, we see that the flux of momentum into Ω through the infinitesimal area da is given by $(\rho v_i)\boldsymbol{v}\cdot(-\boldsymbol{n})da$. Thus the total change $\partial_t P_i^{\text{adv}}(\Omega, t)$ of momentum in Ω due to advection is

$$\partial_t P_i^{\text{adv}} = \int_{\partial\Omega} da(-\boldsymbol{n})\cdot(\rho v_i \boldsymbol{v})$$
$$= -\int_{\partial\Omega} da\, n_j \rho v_i v_j. \quad (26)$$

The rate of momentum change due to pressure is the sum of the pressure force p $(-\boldsymbol{n})da$ from the surroundings on each infinitesimal area da of the surface $\partial\Omega$. Thus, for the ith component of the momentum along the unit vector $\boldsymbol{e}_i$ we obtain

$$\partial_t P_i^{\text{pres}} = \int_{\partial\Omega} da(-\boldsymbol{n})\cdot(p\boldsymbol{e}_i)$$
$$= -\int_{\partial\Omega} da\, n_j p\delta_{ij}. \quad (27)$$

In the last equation we use that $\boldsymbol{n}\cdot\boldsymbol{e}_i = n_j\delta_{ij}$, whereby $\boldsymbol{n}$ can be ascribed the same free index j different from the momentum component index i as in eqn (26).

The momentum in Ω is also changed by viscous friction at the surface $\partial\Omega$ from the surrounding fluid. The frictional force $d\boldsymbol{F}$ on a surface element da with the normal vector $\boldsymbol{n}$ must be characterized by a tensor rank of two as two vectors are involved. This tensor is denoted as the viscous stress tensor σ'_{ij}, and it expresses the ith component of the friction force per area acting on a surface element oriented with its surface normal parallel to the jth unit vector $\boldsymbol{e}_j$. So we have $dF_i = \sigma'_{ij}n_j da$, which

leads directly to the change in the momentum of Ω due to the viscous forces at the surface $\partial\Omega$,

$$\partial_t P_i^{\text{visc}}(\Omega, t) = \int_{\partial\Omega} dF_i = \int_{\partial\Omega} da\, n_j \sigma'_{ij}. \quad (28)$$

The internal friction is only non-zero when fluid particles move relative to each other, hence the viscous stress tensor σ'_{ij} depends only on the spatial derivatives of the velocity. For the small velocity gradients encountered in microfluidics we can safely assume that only first-order derivatives are relevant. Thus, σ'_{ij} must thus depend linearly on the velocity gradients $\partial_i v_j$. Further analysis shows that it must be symmetric, and one way of writing the tensor of rank two satisfying these conditions is[4]

$$\sigma'_{ij} = \eta(\partial_j v_i + \partial_i v_j) + (\beta - 1)\eta(\partial_k v_k)\delta_{ij}, (29)$$

where the first term relates to the dynamic shear viscosity η of an incompressible fluid, and the second term appears when compressibility-induced dilatational viscosity (proportional to $\boldsymbol{\nabla}\cdot\boldsymbol{v}$) cannot be neglected. Here, β ($\approx 5/3$ for water and other simple fluids) is the ratio between the coefficients of the two types of viscosity. The value of η is determined experimentally, and for water we have

$$\eta_{\text{water}}(20\,^\circ\text{C}) = 1.002 \times 10^{-3}\,\text{Pa s}$$
$$= 1.002\,\text{mPa s}. \quad (30)$$

It varies strongly with temperature decreasing from $\eta_{\text{water}}(0\,^\circ\text{C}) = 1.787\,\text{mPa s}$ to $\eta_{\text{water}}(100\,^\circ\text{C}) = 0.282\,\text{mPa s}$.

Combining the results from eqn (23) to (29) yields

$$\int_\Omega d\boldsymbol{r}[(\partial_t\rho)v_i + \rho\partial_t v_i]$$
$$= \int_{\partial\Omega} da\, n_j\Big[-\rho v_i v_j - p\delta_{ij} + \sigma'_{ij}\Big]$$
$$+ \int_\Omega d\boldsymbol{r}\rho g_i. \quad (31)$$

Utilizing Gauss's theorem, the surface integral involving n_j can be rewritten as a volume integral involving ∂_j. Since the resulting volume integral equation is valid for any region Ω the integrands must be identical. After some rewriting we finally arrive at the general equation of motion for the Eulerian velocity field of a viscous fluid,

$$\rho\partial_t v_i + \rho v_j \partial_j v_i = -\partial_i p + \partial_j \sigma'_{ij} + \rho g_i. \quad (32)$$

The left-hand side can be interpreted as inertial force densities, density times the sum of the local and the advective acceleration, while the right-hand side is the sum of intrinsic or applied force densities. Normally, for the so-called Newtonian fluids at a given temperature, the viscosity coefficients η and β can be taken as constants, and eqn (32) reduces to the celebrated Navier–Stokes equation for compressible fluids,

$$\rho[\partial_t v_i + v_j\partial_j v_i] =$$
$$-\partial_i p + \eta\partial_j^2 v_i + \beta\eta\partial_i(\partial_j v_j) + \rho g_i, \quad (33\text{a})$$

$$\rho[\partial_t \boldsymbol{v} + (\boldsymbol{v}\cdot\boldsymbol{\nabla})\boldsymbol{v}] =$$
$$-\boldsymbol{\nabla}p + \eta\nabla^2\boldsymbol{v} + \beta\eta\boldsymbol{\nabla}(\boldsymbol{\nabla}\cdot\boldsymbol{v}) + \rho\boldsymbol{g}. \quad (33\text{b})$$

For incompressible fluids ($\boldsymbol{\nabla}\cdot\boldsymbol{v} = 0$) it becomes

$$\rho[\partial_t \boldsymbol{v} + (\boldsymbol{v}\cdot\boldsymbol{\nabla})\boldsymbol{v}] = -\boldsymbol{\nabla}p + \eta\nabla^2\boldsymbol{v} + \rho\boldsymbol{g}. \quad (34)$$

C. The heat-transfer equation

The third and last governing equation to be established, is the heat-transfer equation, building on the energy density flux and conservation of energy. The thermodynamic quantities for fluids are usually taken per unit mass, directly relating them to the molecules of the fluid. Thus, we work with the internal energy ε per unit mass, the entropy s per unit mass, and the volume $1/\rho$ per unit mass instead of the energy E, the entropy S, and the volume v of the fluid. The first law of thermodynamics relates internal energy $d\varepsilon$, heat Tds, and pressure work $-pd(1/\rho)$, and per unit mass it becomes

$$d\varepsilon = T\,ds - p\,d\left(\frac{1}{\rho}\right) = T\,ds + \frac{p}{\rho^2}d\rho. \quad (35)$$

The densities of the quantities involved are obtained by multiplying them by the mass density ρ, e.g. the energy density is written as $\rho\varepsilon$.

In analogy with the mass and momentum densities above, we consider the rate of change $\partial_t E(\Omega, t)$ of the energy (power conversion) of the fluid inside some fixed region Ω. As the energy density is given by the sum of the kinetic energy density $\frac{1}{2}\rho v^2$ and the internal energy density $\rho\varepsilon$, we obtain

$$\partial_t E = \partial_t \int_\Omega \mathrm{d}\boldsymbol{r} \left[\frac{1}{2}\rho v^2 + \rho\varepsilon \right]$$

$$= \int_\Omega \mathrm{d}\boldsymbol{r}\, \partial_t \left[\frac{1}{2}\rho v^2 + \rho\varepsilon \right]. \qquad (36)$$

Here, E can change by energy advection through the surface $\partial\Omega$ of Ω, by work done by pressure and friction forces from the surroundings acting on the surface $\partial\Omega$, and by heat conduction due to thermal gradients at the surface. For simplicity, we disregard heat sources and sinks that could be present inside Ω, so $\partial_t E$ can be written as

$$\partial_t E = \partial_t E^{\mathrm{adv}} + \partial_t E^{\mathrm{pres}} + \partial_t E^{\mathrm{visc}} + \partial_t E^{\mathrm{cond}}. \qquad (37)$$

The terms $\partial_t \rho$ and $\partial_t v_j$ appearing at the right-hand side of eqn (36) are rewritten using the continuity eqn (21) and the equation of motion eqn (32), whereby

$$\partial_t E = \int_\Omega \mathrm{d}\boldsymbol{r} \left[-\left(\frac{1}{2}v^2 + \varepsilon \right)\partial_j(\rho v_j) \right.$$
$$- \rho v_k \partial_k \left(\frac{1}{2}v^2 \right) - v_j \partial_j p + v_j \partial_k \sigma'_{jk}$$
$$\left. + \rho \partial_t \varepsilon \right. . \qquad (38)$$

The last term $\rho\partial_t\varepsilon$ can be further rewritten by using the first law of thermodynamics (35), thereby bringing the entropy s into play as $\rho\partial_t\varepsilon = \rho T\partial_t s + (p/\rho)\partial_t\rho = \rho T\partial_t s - (p/\rho)\partial_j(\rho v_j)$. Likewise, the third term is rewritten as $-v_j\partial_j p = -\rho v_j\partial_j(\varepsilon + p/\rho) + \rho T v_j\partial_j s$.

Similar to eqn (19) and (26), the advection of energy into the region is easily expressed in terms of the energy flux density $\boldsymbol{J}_\varepsilon = \left(\frac{1}{2}\rho v^2 + \rho\varepsilon \right)\boldsymbol{v}$,

$$\partial_t E^{\mathrm{adv}} = \int_{\partial\Omega} \mathrm{d}a(-\boldsymbol{n})\cdot\boldsymbol{J}_\varepsilon$$
$$= -\int_{\partial\Omega} \mathrm{d}a\, n_j v_j \left[\frac{1}{2}\rho v^2 + \rho\varepsilon \right]. \qquad (39)$$

The power transferred into the region Ω through the work done by the stress forces due to pressure and viscosity at the surface is given by the product of the stress force vector $\sigma_{jk}n_j\mathrm{d}a$ and the velocity of the fluid v_k,

$$\partial_t E^{\mathrm{pres}} + \partial_t E^{\mathrm{visc}} =$$
$$\int_{\partial\Omega} \mathrm{d}a\, n_j \left[-p\delta_{jk} + \sigma'_{jk} \right] v_k. \qquad (40)$$

Thermal conduction occurs in any medium given a spatially varying temperature field $T(\boldsymbol{r})$. The heat flux density $\boldsymbol{J}_{\mathrm{heat}}$, which is the heat-transfer per area per time given in units of $\mathrm{Jm}^{-2}\mathrm{s}^{-1}$ or Wm^{-2}, can therefore be expanded in derivatives of the temperature. For small temperature variations only the first derivative $\boldsymbol{\nabla}T$ is significant, and we arrive at Fourier's law of heat conduction for an isotropic medium,

$$\boldsymbol{J}_{\mathrm{heat}} = -\kappa\boldsymbol{\nabla}T, \qquad (41)$$

where κ is the thermal conductivity of the fluid. For water $\kappa_{\mathrm{water}} = 0.597\ \mathrm{Wm}^{-1}\mathrm{K}^{-1}$ at 20 °C. The rate of change of energy by conduction is readily found through the heat flux density and Fourier's law,

$$\partial_t E^{\mathrm{cond}}(\Omega, t) = \int_{\partial\Omega} \mathrm{d}a(-\boldsymbol{n})\cdot\boldsymbol{J}_{\mathrm{heat}}$$
$$= \int_{\partial\Omega} \mathrm{d}a\, n_j(\kappa\partial_j T). \qquad (42)$$

The heat-transfer equation now follows from eqn (37) using eqn (38), (39), (40), and (42). As before, we use Gauss's theorem to convert the surface integrals into volume integrals, and then equate the integrands to obtain

$$\rho T[\partial_t s + v_j\partial_j s] = \sigma'_{jk}\partial_k v_j + \partial_j[\kappa\partial_j T], \qquad (43a)$$

$$\rho T[\partial_t s + (\boldsymbol{v}\cdot\boldsymbol{\nabla})s] = \boldsymbol{\sigma}' : \boldsymbol{\nabla}\boldsymbol{v} + \boldsymbol{\nabla}\cdot(\kappa\boldsymbol{\nabla}T). \qquad (43b)$$

The left-hand side is ρT times the total time derivative of the entropy per unit mass, hence expressing the total gain in heat density per unit time, while the right-hand side represents the sources for heat gain: viscous friction and thermal conduction.

In microfluidics, the fluid velocities are generally much smaller than the speed of sound in the fluid. Consequently, pressure variations are minute, leading to the constant pressure approximation, for which $\mathrm{d}s = c_\mathrm{p}\mathrm{d}T$, where c_p is the specific heat at constant pressure. In this case the heat-transfer equation reduces to

$$\rho c_\mathrm{p}[\partial_t T + (v_j\partial_j)T] = \partial_j(\kappa\partial_j T) + \sigma'_{jk}\partial_k v_j. (44)$$

For a fluid at rest ($v_j = 0$) with a constant thermal conductivity κ, the equation reduces to the Fourier equation,

$$\partial_t T = D_{\mathrm{th}}\nabla^2 T, \qquad (45)$$

which introduces the thermal diffusivity $D_{\mathrm{th}} = \kappa/(\rho c_p)$. For water the measured value is $D_{\mathrm{th}} = 1.43 \times 10^{-7}\ \mathrm{m}^2\mathrm{s}^{-1}$ at 20 °C.

V. Flow solutions

Mathematically, the richness and beauty of hydrodynamic phenomena are spawned by the non-linear term $\rho(\boldsymbol{v}\cdot\boldsymbol{\nabla})\boldsymbol{v}$ in the Navier–Stokes equation. However, this term is also responsible for complicating the mathematical treatment of the equation; the solutions of the equation have never been fully characterized.

In the following we study two different cases where this complicating non-linear term can be neglected. The first case is the limit of low flow velocities, a limit highly relevant for microfluidic systems. Here, the non-linear term can be neglected as it is much smaller than the viscous term, and we enter the linear regime of the so-called Stokes flow or creeping flow. The second case is when translation symmetry of long, straight channels implies the exact vanishing of the non-linear term. In particular we study the steady-state pressure-driven Poiseuille flow.

A. Hydrostatic pressure

The simplest case is a fluid in mechanical equilibrium. Such a fluid is at rest relative to the walls of the vessel containing it, and the velocity field is therefore trivially zero everywhere, $\boldsymbol{v} = \boldsymbol{0}$. If we let z-axis point upwards, the gravitational acceleration is $\boldsymbol{g} = -g\boldsymbol{e}_z$, and the Navier–Stokes eqn (33b) becomes

$$\boldsymbol{0} = -\boldsymbol{\nabla}p_{\mathrm{hs}} - \rho g\boldsymbol{e}_z, \qquad (46)$$

where the subscript "hs" refers to hydrostatic. For an incompressible fluid, say water, the density ρ is constant and p_{hs} is easily found to be

$$p_{\mathrm{hs}}(z) = p^* - \rho g z, \qquad (47)$$

where p^* is the pressure at the arbitrarily defined zero level $z = 0$. In many microfluidic applications this is the only manifestation of gravity. It is therefore customary to write the total pressure as $p_{\mathrm{tot}} = p + p_{\mathrm{hs}}$, such that in the Navier–Stokes equation the gravitational body force is cancelled by the gradient of hydrostatic pressure. The resulting

Navier–Stokes equation thus contains the auxiliary pressure p and no gravitational body force.

The hydrostatic pressure p_{hs} provides an easy way of generating pressure differences in liquids: the pressure at the bottom of a liquid column of height ΔH is higher by $\Delta p = \rho g \Delta H$ than the pressure at the top. For water $\rho g \approx 10^4$ Pa m^{-1}, so a vertical water column of height 10 cm creates $\Delta p = 1$ kPa, while it takes a height of 10 m to create 10^5 Pa $= 1$ bar ≈ 1 atm.

B. The Reynolds number and the Stokes equation

For small flow velocities the non-linear term is expected to be negligible. To determine the condition for this, we non-dimensionalize the Navier–Stokes equation: all physical variables are expressed in units of characteristic scales. For a system characterized by only one length scale L_0 and one velocity scale V_0, the expression of co-ordinates and velocity in terms of dimensionless co-ordinates and velocity is

$$\boldsymbol{r} = L_0 \tilde{\boldsymbol{r}}, \quad \text{and} \quad \boldsymbol{v} = V_0 \tilde{\boldsymbol{v}}, \qquad (48a)$$

where the tilde indicates a non-dimensionalized quantity, *i.e.* a pure number. Once L_0 and V_0 have been fixed, the scales T_0 and P_0 for time and pressure follow,

$$t = \frac{L_0}{V_0}\tilde{t} = T_0\,\tilde{t}, \quad \text{and} \quad p = \frac{\eta V_0}{L_0}\tilde{p} = P_0\,\tilde{p}. \qquad (48b)$$

Viscosity dominates in microfluidics, so we choose $P_0 = \eta V_0/L_0$ and not as ρV_0^2. By insertion of eqn (48a) and (48b) into the Navier–Stokes eqn (33b) excluding the body-forces as well as the compressibility term, and using the straightforward scaling of the derivatives, $\partial_t = (1/T_0)\tilde{\partial}_t$ and $\nabla = (1/L_0)\tilde{\nabla}$, we obtain

$$p\left[\frac{V_0}{T_0}\tilde{\partial}_t\tilde{\boldsymbol{v}} + \frac{V_0^2}{L_0}(\tilde{\boldsymbol{v}}\cdot\tilde{\nabla})\tilde{\boldsymbol{v}}\right]$$
$$= -\frac{P_0}{L_0}\tilde{\nabla}\tilde{p} + \frac{\eta V_0}{L_0^2}\tilde{\nabla}^2\tilde{\boldsymbol{v}}. \qquad (49)$$

Dividing by $\eta V_0/L_0^2$ this becomes

$$Re\left[\tilde{\partial}_t\tilde{\boldsymbol{v}} + (\tilde{\boldsymbol{v}}\cdot\tilde{\nabla})\tilde{\boldsymbol{v}}\right] = -\tilde{\nabla}\tilde{p} + \tilde{\nabla}^2\tilde{\boldsymbol{v}}, \qquad (50)$$

$$Re \equiv \frac{\rho V_0 L_0}{\eta}, \qquad (51)$$

where the dimensionless parameter Re, the so-called Reynolds number, has been introduced.

For $Re \ll 1$ the left-hand side of eqn (50) can be neglected. For water in microfluidics typical values are $\eta/\rho = 10^{-6}$ m^2 s^{-1}, $L_0 \approx 10^{-4}$ m, and $V_0 \approx 10^{-3}$ m s^{-1}, which leads to a small Reynolds number, $Re \approx 0.1$.

Returning to physical variables in the limit of low Reynolds number, the non-linear Navier–Stokes equation is reduced to the linear Stokes equation,

$$\boldsymbol{0} = -\boldsymbol{\nabla}p + \eta\nabla^2\boldsymbol{v}, \qquad (52)$$

If the time dependence is controlled by some external time scale different from the intrinsic scale $T_0 = L_0/V_0$, the time derivative is not necessarily negligible, and we must employ the time-dependent, linear Stokes equation,

$$\rho\partial_t\boldsymbol{v} = -\boldsymbol{\nabla}p + \eta\nabla^2\boldsymbol{v}. \qquad (53)$$

For zero pressure gradient, and introducing the kinematic viscosity ν, it reduces to a diffusion equation

$$\partial_t\boldsymbol{v} = \nu\nabla^2\boldsymbol{v}, \quad \text{with} \quad \nu = \frac{\eta}{\rho}, \qquad (54)$$

where ν acts as the diffusivity of momentum in the fluid.

An important example of Stokes flow relates to particle solutions. Let an external force move a spherical particle of radius a with velocity $\boldsymbol{v}_p$ through a fluid that itself moves with velocity $\boldsymbol{v}$ far from the particle. Given the no-slip boundary condition on the particle surface $\partial\Omega_p$, the velocity and pressure field of the fluid can be found from eqn (52), and from that

follows the viscous Stokes drag $\boldsymbol{F}_{drag}$ on the particle,[4]

$$\boldsymbol{F}_{drag} = \int_{\partial\Omega_p} da(-p\boldsymbol{n} + \sigma'\cdot\boldsymbol{n})$$
$$= 6\pi\eta a(\boldsymbol{v} - \boldsymbol{v}_p). \qquad (55)$$

Changing the particle concentration from zero to a few volume percent does not affect the flow profile significantly, while the viscosity may increase by a few percent.

C. Poiseuille flow

Our prime example of a solution to the Navier–Stokes equation in the dynamic case, is the pressure-driven, steady-state flow in a straight channel, also known as Poiseuille flow, see Fig. 3. This class of flow is of major importance for the basic understanding of liquid handling in microfluidic lab-on-a-chip systems.

In a Poiseuille flow the fluid is driven through a long, straight, and rigid channel of length L by imposing a pressure difference, Δp, between the two ends of the channel. The channel is placed horizontally along the x-axis, so along the z-axis gravity is balanced by the hydrostatic pressure. Furthermore, the cross-section of the channel is constant along the x-axis, so the liquid in the channel is only affected by the force from the pressure drop along the x-axis. The velocity field is therefore assumed to have only an x-component, and this component depends only on the transverse coordinates y and z, such that $\boldsymbol{v} = v_x(y, z)\boldsymbol{e}_x$. This implies $(\boldsymbol{v}\cdot\boldsymbol{\nabla})\boldsymbol{v} = (v_x\partial_x)v_x(y, z)\boldsymbol{e}_x = \boldsymbol{0}$, and the non-linear Navier–Stokes equation becomes the linear Stokes equation.

For the velocity field we employ the so-called no-slip boundary condition: On all points on the solid surface $\partial\Omega$ the velocity
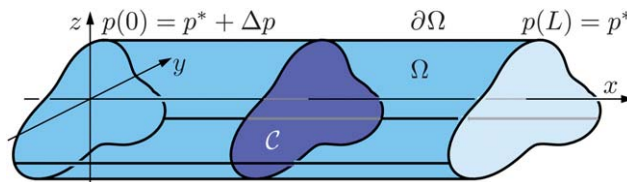

Fig. 3 Poiseuille flow of liquid through a straight channel Ω (blue), where the flow is subject to the no-slip boundary condition on the surface $\partial\Omega$. The channel is translational invariant in the x direction, and it has an arbitrarily shaped cross-section $\mathcal{C}$ (dark blue) in the yz-plane. The pressure at $x = 0$ (left) is Δp higher than at $x = L$ (right).

of the fluid equals that of the wall v_{wall} (often equal to zero),

$$v(r) = v_{wall}, \text{ for } r \in \partial\Omega \text{ (no-slip)}. \quad (56)$$

The microscopic origin of this condition is the assumption of complete momentum relaxation between the molecules of the wall and the outermost molecules of the fluid that collide with the wall. The momentum is relaxed on a length scale, which approximately is the molecular mean free path in the fluid, which for liquids means one intermolecular distance ($\simeq 0.3$ nm).

The final form of the steady-state Navier–Stokes equation for the Poiseuille flow thus becomes

$$v(r) = v_x(y, z)e_x, \quad (57a)$$

$$0 = -\nabla p + \eta\nabla^2[v_x(y, z)e_x]. \quad (57b)$$

Since the y and z components of the velocity field are zero, it follows that both $\partial_y p$ and $\partial_z p$ are zero, and consequently the pressure field depends only on x, $p(r) = p(x)$. Using this result, the x component of the Navier–Stokes eqn (57b) becomes

$$\eta[\partial_y^2 + \partial_z^2]v_x(y, z) = \partial_x p(x). \quad (58)$$

Here, it is seen that the left-hand side is a function of y and z, while the right-hand side is a function of x. Therefore, the only possible solution is that the two sides of the Navier–Stokes equation equal the same constant. However, a constant pressure gradient $\partial_x p(x)$ implies that the pressure must be a linear function of x, and using the boundary conditions for the pressure we obtain

$$p(r) = \frac{\Delta p}{L}(L - x) + p^*. \quad (59)$$

With this we arrive at the second-order partial differential equation for $v_x(y, z)$ in the cross-section $\mathcal{C}$ obeying no-slip boundary conditions at the solid walls $\partial\Omega$,

$$\left[\partial_y^2 + \partial_z^2\right]v_x(y, z) = -\frac{\Delta p}{\eta L}, \text{ for } (y, z) \in \mathcal{C} \quad (60a)$$

$$v_x(y, z) = 0, \text{ for } (y, z) \in \partial\Omega. \quad (60b)$$

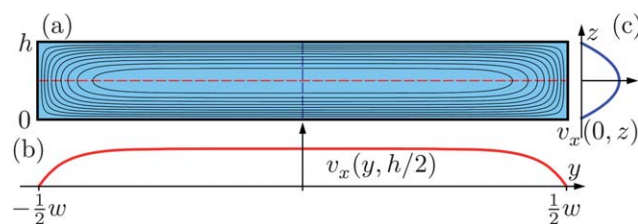The resulting velocity field can be determined analytically for a limited

Fig. 4 (a) Contour lines for the velocity field $v_x(y, z)$ for a Poiseuille-flow in a rectangular channel. The contour lines are shown in steps of 10% of the maximal value $v_x(0, h/2)$. (b) A plot (red) of $v_x(y, h/2)$ along the long centerline. (c) A plot (blue) of $v_x(0, z)$ along the short centerline.

number of cross-section shapes, as done in ref. 4. Here, we present three of these solutions: a circular cross-section of radius a; the space between two horizontal infinite parallel plates placed at $z = 0$ and $z = h$; and a rectangular cross-section $-\frac{1}{2}w < y < \frac{1}{2}w$ and $0 < z < h$, see Fig. 4(a),

$$v_x(y, z) = \frac{\Delta p}{4\eta L}(a^2 - y^2 - z^2), \text{ circular tube}, \quad (61a)$$

$$v_x(y, z) = \frac{\Delta p}{2\eta L}(h - z)z, \text{ parallel plates}, \quad (61b)$$

$$v_x(y, z)$$
$$= \frac{4h^2\Delta p}{\pi^3\eta L}\sum_{n,\text{odd}}^{\infty}\frac{1}{n^3}\left[1 - \frac{\cosh\left(n\pi\frac{y}{h}\right)}{\cosh\left(n\pi\frac{w}{2h}\right)}\right]$$
$$\sin\left(n\pi\frac{z}{h}\right), \text{ rectangular cross-section, } h < w. \quad (61c)$$

Inspection shows that these solutions are correct. Note how the flow profile in the rectangular case is independent of y along a large part $w - h$ of the long width, Fig. 4 (b), but parabolic across the short height, Fig. 4(c).

D. Flow rate

Once the velocity field is determined, it is possible to calculate the so-called volumetric flow rate Q, which is defined as the fluid volume discharged by the channel per unit time. In the case of the geometry of Fig. 3 we have

$$Q = \int_{\mathcal{C}} dy\,dz\,v_x(y, z) = \mathcal{A}v_{\text{avr}}, \quad (62)$$

where $v_{\text{avr}} = (1/\mathcal{A})\int_{\mathcal{C}} dy\,dz\,v_x(y, z)$ is the average velocity and $\mathcal{A}$ is the cross-section area. The flow rate for three selected Poiseuille flows are

$$Q = \frac{\pi a^4}{8\eta L}\Delta p, \text{ circular tube}, \quad (63a)$$

$$Q = \frac{h^3 w}{12\eta L}\Delta p, \text{ parallel-plates}, \quad (63b)$$

$$Q \approx \left[1 - 0.630\frac{h}{w}\right]\frac{h^3 w}{12\eta L}\Delta p,$$
$$\text{rectangular, } h < w. \quad (63c)$$

For the Poiseuille flow in a rectangular channel of height h and width w, an analytical solution in closed form has not yet been found. However, the error of the approximate result (63c) is just 13% for the worst case (a square with $h = w$), while already for an aspect ratio of a half (a rectangle with $h = w/2$) it has decreased to 0.2%.

The SI unit of flow rate is m³ s⁻¹, but in microfluidics volume is often measured in μL = mm³ and time in minutes, so the following conversion factors are useful,

$$1\frac{\mu L}{s} = 10^{-9}\frac{m^3}{s}, \quad 1\frac{\mu L}{min} = 1.67 \times 10^{-11}\frac{m^3}{s}. \quad (64)$$

VI. Equivalent circuit modeling

Often it suffices to find the flow rate through a given microfluidic network rather than the detailed flow field. To this end the method of equivalent circuit modeling may be used. This type of modeling is only strictly valid for steady Stokes flow in the limit of zero velocity, however, it is a good

approximation for $Re \lesssim 1$ in long, narrow channels, for which entrance effects are negligible, and for changes propagating slower than the speed of sound.

$$[Q] = \frac{m^3}{s}, \quad [\Delta p] = \text{Pa} = \frac{kg}{m\,s^2},$$

$$[R_{\text{hyd}}] = \frac{\text{Pa s}}{m^3} = \frac{kg}{m^4\,s}. \quad (66)$$

A. Hydraulic resistance

Above we have found that a constant pressure drop Δp results in a constant flow rate Q. This result can be summarized in the Hagen–Poiseuille law

$$\Delta p = R_{\text{hyd}}Q, \quad \text{or} \quad R_{\text{hyd}} = \frac{\Delta p}{Q}, \quad (65)$$

where we have introduced the proportionality factor R_{hyd} known as the hydraulic resistance; a central concept in characterizing and designing microfluidic channels in lab-on-a-chip systems, see the list in Table 1. The SI units used in the Hagen–Poiseuille law are

The Hagen–Poiseuille law is analogous to Ohm's law, $\Delta U = RI$, for a wire carrying the electrical current I and having the electrical resistance R and the potential drop ΔU. In hydraulic systems volume is moved and Q is volume per time, while in electric systems charge is moved and I is charge per time. Likewise, Δp is energy per volume as ΔU is energy per charge. Hydraulic power is $Q\Delta P$ (vol/time × energy/vol) while electric power is $I\Delta U$ (charge/time × energy/charge). For low Reynolds numbers fluid flow is described by the linear Stokes equation, and to a good approximation the hydraulic resistances obey the same rules for series and parallel coupling as the electric resistances in linear circuit theory. Thus for two hydraulic resistance R_1 and R_2 we have

$$R_{\text{hyd}}^{\text{series}} = R_1 + R_2, \quad (67a)$$

and $$R_{\text{hyd}}^{\text{parallel}} = \left(\frac{1}{R_1} + \frac{1}{R_2}\right)^{-1}. \quad (67b)$$

For a generic fluidic network Kirchhoff's laws apply:

a) The sum of mass flow rates entering/leaving any node in the circuit is zero.
b) The sum of all pressure differences in any closed loop of the circuit is zero.
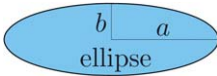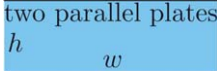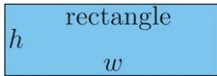
$$(68)$$

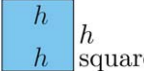## B. Hydraulic compliance

The analogy between hydraulic and electric systems can be taken one step further. When the pressure increases by Δp in a liquid inside an elastic channel, the volume available to the liquid increases by ΔV. This is analogous to the charging of a capacitor where in increase an voltage by ΔU increases the charge on the capacitor by $\Delta q = C\Delta U$. The electric capacitance is given by $C = \partial q/\partial U$, and we are led to introduce hydraulic capacitance C_{hyd}, also known as compliance, given by

$$C_{\text{hyd}} = \frac{dV}{dp}, \quad \text{with} \quad [C_{\text{hyd}}] = \text{m}^3\,\text{Pa}^{-1}. \quad (69)$$

As an example of compliance we consider a simple model of a soft-walled channel filled with an incompressible liquid as sketched in Fig. 5(a). If the pressure increases inside the channel, the latter will expand. The compliance C_{hyd} of the channel is a given constant related to the geometry and the material properties of the channel walls. As a simplification we model the channel as consisting of two subchannels with hydraulic resistances R_1 and R_2, respectively, connected in series. The pressure, p_c, at the point where the two subchannels connect determines the expansion of the whole channel. The equivalent model is seen in Fig. 5(b). We let the pressure at the inlet be p^* for time

Table 1 The hydraulic resistance for water flowing through straight channels with different cross-sectional shapes. The numerical values are calculated using $\eta = 1$ mPa s, $L = 1$ m, $a = 100$ µm, $b = 33$ µm, $h = 100$ µm, and $w = 300$ µm. Note that the areas are different

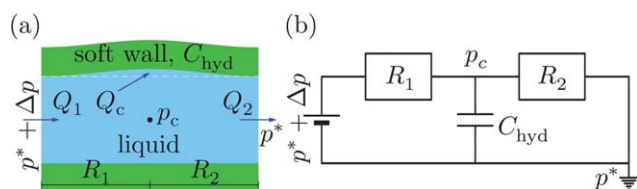| Shape and parameters	R_{hyd} expression	$R_{\text{hyd}}\left[10^{12}\frac{\text{Pa s}}{m^3}\right]$
circle (a)	$\dfrac{8}{\pi}\eta L\dfrac{1}{a^4}$	25
ellipse (b, a)	$\dfrac{4}{\pi}\eta L\dfrac{1 + (b/a)^2}{(b/a)^3}\dfrac{1}{a^4}$	393
triangle (a, a, a)	$\dfrac{320}{\sqrt{3}}\eta L\dfrac{1}{a^4}$	1850
two parallel plates (h, w)	$12\eta L\dfrac{1}{h^3 w}$	40
rectangle (h, w)	$\dfrac{12\eta L}{1 - 0.63(h/w)}\dfrac{1}{h^3 w}$	51
square (h, h, h)	$28.4\,\eta L\dfrac{1}{h^4}$	284
parabola (h, w)	$\dfrac{105}{4}\eta L\dfrac{1}{h^3 w}$	88
perimeter $\mathcal{P}$, area $\mathcal{A}$	$\approx 2\eta L\dfrac{\mathcal{P}^2}{\mathcal{A}^3}$	—

Fig. 5 (a) Compliance in a soft-walled channel (green) filled with liquid (light blue). The liquid center pressure is denoted by p_c, while R_1 and R_2 denote the hydraulic resistances of the first and second part of the channel, respectively. Mass conservation yields $Q_1 = Q_2 + Q_c$. (b) The equivalent circuit diagram corresponding to the soft-walled channel of panel (a), where R_1 and R_2 are the hydraulic resistances of each part of the channel, while C_{hyd} is the compliance of the soft wall.

$t < 0$ and $p^* + \Delta p$ for time $t > 0$. The flow rate at the inlet and the outlet are given by the Hagen–Poiseuille law $Q_1 = (p^* + \Delta p - p_c)/R_1$ and $Q_2 = (p_c - p^*)/R_2$, respectively, while the rate of volume expansion inside the chamber is given by $Q_c = \partial_t V = C_{hyd}\partial_t p_c$. Since the liquid is assumed to be incompressible, conservation of mass leads to $Q_1 = Q_2 + Q_c$, and we arrive at a differential equation for the liquid center pressure p_c,

$$\partial_t p_c = -\left(\frac{1}{\tau_1} + \frac{1}{\tau_2}\right)p_c + \left(\frac{1}{\tau_1} + \frac{1}{\tau_2}\right)p^* + \frac{1}{\tau_1}\Delta p,$$

(70)

where $\tau_1 = R_1 C_{hyd}$ and $\tau_2 = R_2 C_{hyd}$ are the hydraulic RC times. The solution,

$$p_c(t) = p^* + \left(1 - \exp[\tau_1^{-1} + \tau_2^{-1}]t\right) \times \frac{\tau_2}{\tau_1 + \tau_2}\Delta p,$$

(71)

is analogous to the voltage across a capacitor being charged through a voltage divider.

Often the external tubing may lead to long transient times in the external system due to the RC-time

$$\tau_{RC} = R_{hyd}C_{hyd}$$

(72)

arising from the hydraulic resistance R_{hyd} and compliance C_{hyd}. For an elastic tube of fixed length L, inner radius a, wall thickness d, and thickness ratio $\delta = d/a$, C_{hyd} can be derived from basic theory of elasticity,[38]

$$C_{hyd}^{tube} = 2\pi(1 + \bar{v})\frac{(1 - 2\bar{v}) + (1 + \delta)^2}{(1 + \delta)^2 - 1}\frac{a^2 L}{Y}.$$

(73)

Here, $\bar{v}$ is the Poisson ratio, and Y is Young's modulus. Specific examples of transient RC times are listed in Table 2.

If a gas bubble is trapped inside a microfluidic channel, an extra compliance C_{hyd}^{bubble} is added to the system,

$$C_{hyd}^{bubble} = \frac{dV}{dp} = -\frac{dV^{bubble}}{dp} = \frac{4\pi}{3}\frac{a^3}{p^*}.$$

(74)

Here, we have assumed isothermal compression of the gas bubble around ambient pressure p^*. For isentropic compression the hydraulic compliance is multiplied by the adiabatic factor $\gamma \approx 1.4$. A large bubble with $a = 1$ mm leads to $C_{hyd}^{bubble} = 42 \times 10^{-15}$ m^3 Pa^{-1}, comparable to the silicone tube in Table 2.

C. Hydraulic inductance

The last analogy is inductance. The self-inductance L_{el}, or the electric inertia, is the ability of an electric system to maintain a given current I. A rate of change $\partial_t I$ in the current induces a potential drop $\Delta U = L_{el}\partial_t I$. Hydraulic inductance L_{hyd} therefore relates to maintaining an existing volume current $Q = \mathcal{A}v_{avr}$. Since the rate of change $\partial_t Q = \mathcal{A}\partial_t v_{avr}$ involves acceleration, L_{hyd} must correspond to inertia.

Consider the flow through a channel of length L and cross-section area $\mathcal{A}$. If the force F driving the flow arises from a pressure drop Δp, we find from Newton's second law that

$\Delta p = F/\mathcal{A} = (\rho L\mathcal{A})\partial_t v_{avr}/\mathcal{A}$. This leads to $\Delta p = (\rho L/\mathcal{A})\partial_t Q$, from which we can read off the hydraulic inductance L_{hyd} as

$$L_{hyd} = \frac{\rho L}{\mathcal{A}}, \quad \text{with} \quad [L_{hyd}] = \frac{\text{Pa s}^2}{\text{m}^3}. \quad (75)$$

In analogy with the RC-time, there is also a transient RL-time given by $\tau_{RL} = L_{hyd}/R_{hyd}$. For a tube it is

$$\tau_{RL}^{tube} = \frac{L_{hyd}}{R_{hyd}} = \frac{\rho a^2}{8\eta} = \frac{a^2}{8\nu}, \quad (76)$$

where in the last equality we have used the kinematic viscosity ν from eqn (54). Specific examples of RL times are listed in Table 2. For a more complete example of circuit modeling in a microfluidic system with pulsatile flow including compliance and air bubbles see ref. 39.

VII. Concluding remarks

In this tutorial paper we have established the theoretical framework for the continuum description of fluids, and based on conservation laws, we have derived the governing equations in microfluidics. Some important, basic flow solutions to the these equations have been presented and analyzed in terms of equivalent circuit modeling, introducing the concepts of hydraulic resistance, compliance, and inductance. The theory presented here does not only apply to the fluid flow, it is also the starting point for the ultrasound acoustics to be treated in the following tutorial paper.

Acknowledgements

Table 2 The hydraulic resistance R_{hyd}, compliance C_{hyd}, and inductance L_{hyd} as well as the RC and RL times (τ_{RC} and τ_{RL}) for water ($\eta = 1$ mPa s, $\rho = 998$ kg m^{-3}) in a straight circular channel (length $L = 1$ m, radius $a = 0.1$ mm, thickness ratio $\delta = 1$) made of either soft silicone rubber ($Y = 2.1$ MPa, $\bar{v} = 0.49$) or hard teflon ($Y = 0.5$ GPa, $\bar{v} = 0.45$). It takes 0.7 ms for a pressure wave to propagate through the channel

Material	$R_{hyd}\left[10^{12}\frac{\text{Pa s}}{\text{m}^3}\right]$	$C_{hyd}\left[10^{-15}\frac{\text{m}^3}{\text{Pa}}\right]$	$L_{hyd}\left[10^9\frac{\text{Pa s}^2}{\text{m}^3}\right]$	τ_{RC} [ms]	τ_{RL} [ms]
Silicone	25	60	32	1500	1.3
Teflon	25	0.25	32	6.2	1.3

References

1 P. Tabeling, *Introduction to Microfluidics*, Oxford University Press, Oxford, 2005.

2 G. Karniadakis, A. Beskok and N. Aluru, *Microflows and Nanoflows: Fundamentals and Simulation*, Springer Science + Business Media, Inc., New York NY, 2005.

3 N.-T. Nguyen and S. T. Wereley, *Fundamentals and Applications of Microfluidics*, Artech House, Norwood MA, 2nd edn, 2006.

4 H. Bruus, *Theoretical Microfluidics*, Oxford University Press, Oxford, 2008.

5 J. Berthier and P. Silberzan, *Microfluidics for Biotechnology*, Artech House, Norwood MA, 2nd edn, 2010.

6 B. Kirby, *Micro- and Nanoscale Fluid Mechanics: Transport in Microfluidic Devices*, Cambridge University Press, New York, 2010.

7 A. J. Mach and D. Di Carlo, *Biotechnol. Bioeng.*, 2010, **107**, 302–311.

8 S. Jacobson, R. Hergenroder, L. Koutny and J. Ramsey, *Anal. Chem.*, 1994, **66**, 1114–1118.

9 P. R. C. Gascoyne, J. Noshari, T. J. Anderson and F. F. Becker, *Electrophoresis*, 2009, **30**, 1388–1398.

10 M. Gijs, *Microfluidics Nanofluidics*, 2004, **1**, 22–40.

11 L. Huang, E. Cox, R. Austin and J. Sturm, *Science*, 2004, **304**, 987–990.

12 D. Johnson and D. Feke, *Sep. Technol.*, 1995, **5**, 251–258.

13 K. Yasuda, S. Umemura and K. Takeda, *Jpn. J. Appl. Phys.*, 1995, **34**, 2715–2720.

14 J. J. Hawkes and W. T. Coakley, *Sens. Actuators, B*, 2001, **75**, 213–222.

15 J. J. Hawkes, W. T. Coakley, M. Groschl, E. Benes, S. Armstrong, P. J. Tasker and H. Nowotny, *J. Acoust. Soc. Am.*, 2002, **111**, 1259–1266.

16 N. R. Harris, M. Hill, S. Beeby, Y. Shen, N. M. White, J. J. Hawkes and W. T. Coakley, *Sens. Actuators, B*, 2003, **95**, 425–434.

17 F. Petersson, A. Nilsson, C. Holm, H. Jönsson and T. Laurell, *Analyst*, 2004, **129**, 938–43.

18 F. Petersson, A. Nilsson, C. Holm, H. Jönsson and T. Laurell, *Lab Chip*, 2005, **5**, 20–2.

19 J. Hultström, O. Manneberg, K. Dopf, H. M. Hertz, H. Brismar and M. Wiklund, *Ultrasound Med. Biol.*, 2007, **33**, 145–151.

20 M. Evander, L. Johansson, T. Lilliehorn, J. Piskur, M. Lindvall, S. Johansson, M. Almqvist, T. Laurell and J. Nilsson, *Anal. Chem.*, 2007, **79**, 2984–2991.

21 J. Svennebring, O. Manneberg, P. Skafte-Pedersen, H. Bruus and M. Wiklund, *Biotechnol. Bioeng.*, 2009, **103**, 323–328.

22 A. Lenshof, A. Ahmad-Tajudin, K. Jaras, A.-M. Sward-Nilsson, L. Aberg, G. Marko-Varga, J. Malm, H. Lilja and T. Laurell, *Anal. Chem.*, 2009, **81**, 6030–6037.

23 J. V. Norris, M. Evander, K. M. Horsman-Hall, J. Nilsson, T. Laurell and J. P. Landers, *Anal. Chem.*, 2009, **81**, 6089–6095.

24 C. Grenvall, P. Augustsson, J. R. Folkenberg and T. Laurell, *Anal. Chem.*, 2009, **81**, 6195–6200.

25 T. Franke, S. Braunmueller, L. Schmid, A. Wixforth and D. A. Weitz, *Lab Chip*, 2010, **10**, 789–794.

26 P. Thevoz, J. D. Adams, H. Shea, H. Bruus and H. T. Soh, *Anal. Chem.*, 2010, **82**, 3094–3098.

27 P. Augustsson, R. Barnkob, C. Grenvall, T. Deierborg, P. Brundin, H. Bruus and T. Laurell, *Proc. 14th MicroTAS, 3–7 October 2010, Groningen, The Netherlands*, 2010, pp. 1337–39.

28 S. M. Hagsäter, T. G. Jensen, H. Bruus and J. P. Kutter, *Lab Chip*, 2007, **7**, 1336–1344.

29 J. Shi, H. Huang, Z. Stratton, Y. Huang and T. J. Huang, *Lab Chip*, 2009, **9**, 3354–3359.

30 O. Manneberg, S. M. Hagsäter, J. Svennebring, H. M. Hertz, J. P. Kutter, H. Bruus and M. Wiklund, *Ultrasonics*, 2009, **49**, 112–119.

31 O. Manneberg, B. Vanherberghen, B. Onfelt and M. Wiklund, *Lab Chip*, 2009, **9**, 833–837.

32 P. Glynne-Jones, R. J. Boltryk, N. R. Harris, A. W. J. Cranny and M. Hill, *Ultrasonics*, 2010, **50**, 68–75.

33 J. D. Adams, P. Thevoz, H. Bruus and H. T. Soh, *Appl. Phys. Lett.*, 2009, **95**, 254103–1.

34 S. Oberti, D. Moeller, A. Neild, J. Dual, F. Beyeler, B. J. Nelson and S. Gutmann, *Ultrasonics*, 2010, **50**, 247–257.

35 R. Barnkob, P. Augustsson, T. Laurell and H. Bruus, *Lab Chip*, 2010, **10**, 563–570.

36 P. Augustsson, R. Barnkob, S. T. Wereley, H. Bruus and T. Laurell, *Lab Chip*, 2011, DOI: 10.1039/c1lc20637k.

37 H. Bruus, *Lab Chip*, 2011, DOI: 10.1039/c1lc20770a.

38 L. D. Landau and E. M. Lifshitz, *Theory of Elasticity, 3rd Edition. Course of Theoretical Physics*, Pergamon Press, Oxford, 1986, vol. 7.

39 S. Vedel, L. H. Olesen and H. Bruus, *J. Micromech. Microeng.*, 2010, **20**, 035026.